

The 1^2A_1 , 1^2B_2 , and 1^2A_2 states of the SO_2^+ ion studied using multiconfiguration second-order perturbation theory

Wen-Zuo Li, Ming-Bao Huang, and Bo-Zhen Chen

Citation: *The Journal of Chemical Physics* **120**, 4677 (2004); doi: 10.1063/1.1645244

View online: <http://dx.doi.org/10.1063/1.1645244>

View Table of Contents: <http://aip.scitation.org/toc/jcp/120/10>

Published by the American Institute of Physics



SciLight

Sharp, quick summaries illuminating
the latest physics research

Sign up for **FREE!**

AIP
Publishing

The 1^2A_1 , 1^2B_2 , and 1^2A_2 states of the SO_2^+ ion studied using multiconfiguration second-order perturbation theory

Wen-Zuo Li, Ming-Bao Huang,^{a)} and Bo-Zhen Chen

Department of Chemistry, Graduate School, Chinese Academy of Sciences, P.O. Box 3908, Beijing 100039, People's Republic of China

(Received 6 November 2003; accepted 10 December 2003)

The 1^2A_1 , 1^2B_2 , and 1^2A_2 electronic states of the SO_2^+ ion have been studied using multiconfiguration second-order perturbation theory (CASPT2) and two contracted atomic natural orbital basis sets, $S[6s4p3d1f]/O[5s3p2d1f]$ (ANO-L) and $S[4s3p2d]/O[3s2p1d]$ (ANO-S), and the three states were considered to correspond to the observed \tilde{X} , \tilde{B} , and \tilde{A} states, respectively, in the previous experimental and theoretical studies. Based on the CASPT2/ANO-L adiabatic excitation energy calculations, the \tilde{X} , \tilde{A} , and \tilde{B} states of SO_2^+ are assigned to 1^2A_1 , 1^2B_2 , and 1^2A_2 , respectively, and our assignments of the \tilde{A} and \tilde{B} states are contrary to the previous assignments (\tilde{A} to 2A_2 and \tilde{B} to 2B_2). The CASPT2/ANO-L energetic calculations also indicate that the 1^2A_1 , 1^2B_2 , and 1^2A_2 states are, respectively, the ground, first excited, and second excited states at the ground-state (1^2A_1) geometry of the ion and at the geometry of the ground-state SO_2 molecule. Based on the CASPT2/ANO-L results for the geometries, we realize that the experimental geometries (determined by assuming the bond lengths to be the same as the neutral ground state of SO_2) were not accurate. The CASPT2/ANO-S calculations for the potential energy curves as functions of the OSO angle confirm that the 1^2B_2 and 1^2A_2 states are the results of the Renner–Teller effect in the degenerate $^2\Pi_g$ state at the linear geometry, and it is clearly shown that the 1^2B_2 curve, as the lower component of the Renner splitting, lies below the 1^2A_2 curve. The UB3LYP/cc-pVTZ adiabatic excitation energy calculations support the assignments (\tilde{A} to 2B_2 and \tilde{B} to 2A_2) based on the CASPT2/ANO-L calculations. © 2004 American Institute of Physics. [DOI: 10.1063/1.1645244]

I. INTRODUCTION

The sulfur dioxide ion (SO_2^+) plays an important role in atmospheric chemistry.¹ Numerous experimental studies have been devoted to the SO_2^+ ion, including photoelectron spectroscopy,^{2,3} electron impact ionization,⁴ photoionization,^{5,6} photodissociation spectrum,⁷ and photo-fragment excitation spectrum.⁸ Based on the resolutions of the photoelectron spectra (see Ref. 2, and references therein), the \tilde{X} state of SO_2^+ is in the first band and the \tilde{A} and \tilde{B} states are in the second band. The first and second bands are close in energy and the third band is at least 2.5 eV higher in energy than the second band. In the present theoretical work we have studied the three lowest-lying electronic states (\tilde{X} , \tilde{A} , and \tilde{B}) of the SO_2^+ ion.

The experimental adiabatic ionization potential (AIP) values for the \tilde{X} , \tilde{A} , and \tilde{B} states of SO_2^+ were reported to be 12.35, 12.99, and 13.34 eV by Wang *et al.*,² and similar values were reported by Holland *et al.*³ The adiabatic excitation energy (T_0) values for the SO_2^+ ion are considered to be equal to the differences between the AIP values for excited states and the AIP value for the ground state, and therefore the (experimental) T_0 values for the \tilde{A} and \tilde{B} states of SO_2^+ are 0.64 and 0.99 eV, respectively, evaluated using the AIP

values of Wang *et al.*² The observed vibrational frequencies⁷ for the ν_1 and ν_2 modes were reported to be around 1151 and 454 cm^{-1} in the \tilde{X} state and to be around 953 and 499 cm^{-1} in the \tilde{A} state, respectively (frequencies for the ν_3 mode were not reported). Experimental geometries for the \tilde{X} and \tilde{A} states were found in the literature and the S–O bond length and the OSO bond angle were reported to be 1.432 Å and 136.5° for the \tilde{X} state and to be 1.432 Å and 102.5° for the \tilde{A} state, respectively.⁹ We note in Ref. 9 that in determination of the geometries for the \tilde{X} and \tilde{A} states the bond lengths were assumed to be the same (1.432 Å) as the neutral ground state of SO_2 . Experimental geometric parameters and frequencies for the \tilde{B} state are not available. In all the experimental papers,^{2–9} the \tilde{X} , \tilde{A} , and \tilde{B} states of the SO_2^+ ion were assigned to 1^2A_1 , 1^2A_2 , and 1^2B_2 , respectively. These assignments were based on the energy ordering of the three highest occupied molecular orbitals ($\dots 5b_2^2 1a_2^2 8a_1^2$) in the electronic structure of the ground-state SO_2 molecule.

Theoretical studies should be able to assign the observed electronic states of the SO_2^+ ion and accurate calculations should be able to reproduce the experimental data (for example, geometric and energetic data for the ground and excited states). To our knowledge, there are only two theoretical (*ab initio*) papers on electronic states of the SO_2^+ ion^{10,11} in the literature, and both were published in 1970s. Hillier and Saunders¹⁰ performed *ab initio* restricted Hartree–Fock

^{a)} Author to whom all correspondence should be addressed; electronic mail: mbhuang1@gscas.ac.cn

(RHF) calculations for electronic states of SO_2^+ . Their calculated AIP values for the $(1)^2A_1$, $(1)^2A_2$, and $(1)^2B_2$ states of SO_2^+ were 11.84, 11.94, and 12.88 eV, respectively, which indicated that the 1^2A_1 , 1^2A_2 , and 1^2B_2 states corresponded to the \tilde{X} , \tilde{A} , and \tilde{B} states, respectively, and the calculated equilibrium geometries were also reported.¹⁰ Cederbaum *et al.*¹¹ performed Green's function calculations for the vertical ionization potentials for the three lowest-lying states of SO_2^+ . Their "final" calculation results indicated that at the geometry of the ground-state SO_2 molecule the three lowest-lying states of SO_2^+ were 2A_1 , 2A_2 , and 2B_2 , in an increasing order of energy. These two theoretical papers supported the assignments (\tilde{X} to 1^2A_1 , \tilde{A} to 1^2A_2 , and \tilde{B} to 1^2B_2) presented in the experimental papers.²⁻⁹

It is known that the CASSCF (complete active space self-consistent field)¹² and CASPT2 (multiconfiguration second-order perturbation theory)^{13,14} methods are effective for theoretical studies of excited electronic states of molecules. We have studied the 1^2A_1 , 1^2B_2 , and 1^2A_2 states of the SO_2^+ ion by using the CASPT2 method, and in the present article we will present our assignments of the \tilde{X} , \tilde{A} , and \tilde{B} states of the SO_2^+ ion based on our CASPT2 calculations. We will report the CASPT2 results for the 1^2A_1 , 1^2B_2 , and 1^2A_2 states, which include equilibrium geometries, adiabatic excitation energies, vertical excitation energies, and potential energy curves, and we will compare the results with available experimental data for the \tilde{X} , \tilde{A} , and \tilde{B} states. We also performed the CASSCF and density functional theory (DFT) UB3LYP calculations for the 1^2A_1 , 1^2B_2 , and 1^2A_2 states.

II. CALCULATION DETAILS

We performed the CASPT2, CASSCF, and UB3LYP calculations for the 1^2A_1 , 1^2B_2 , and 1^2A_2 states of the SO_2^+ ion, though the main conclusions of the present study will be drawn on the basis of the CASPT2 calculation results. For confirming that the 1^2A_1 , 1^2B_2 , and 1^2A_2 states are the three lowest-lying states of the ion, we also performed CASPT2 energetic calculations for some higher-lying states (see Sec. III).

The CASSCF and CASPT2 calculations were carried out using the MOLCAS 5.2 quantum-chemistry software.¹⁵ With a CASSCF wave function constituting the reference function the CASPT2 calculations were performed to compute the first-order wave function and the second-order energy in the full-CI space. In the CAS calculations we used two contracted atomic natural orbital (ANO) basis sets,¹⁶⁻¹⁸ $S[6s4p3d1f]/O[5s3p2d1f]$ and $S[4s3p2d]/O[3s2p1d]$, denoted as ANO-L and ANO-S, respectively.

The equilibrium geometries of the 1^2A_1 , 1^2B_2 , and 1^2A_2 states were predicted by performing the CASSCF/ANO-L geometry optimization calculations and by the CASPT2/ANO-L stepwise geometry optimization calculations. The vibrational frequencies in the three states were calculated only at the CASSCF/ANO-L level. Based on the CASPT2/ANO-L energies of the three states calculated at the respective geometries optimized at the CASSCF/ANO-L, CASPT2/ANO-L, and UB3LYP/cc-pVTZ (see the follow-

ing) levels, we obtained the CASPT2/ANO-L//CASSCF/ANO-L, CASPT2/ANO-L//CASPT2/ANO-L, and CASPT2/ANO-L//UB3LYP/cc-pVTZ (abbreviated to "CASPT2//CASSCF," "CASPT2//CASPT2," and "CASPT2//UB3LYP," respectively) adiabatic excitation energy (T_0) values for the three states. Based on the CASPT2/ANO-L energies of the three states calculated at the CASSCF/ANO-L, CASPT2/ANO-L, and UB3LYP/cc-pVTZ optimized geometries of the 1^2A_1 (\tilde{X}^2A_1) state, we obtained the CASPT2//CASSCF, CASPT2//CASPT2, and CASPT2//UB3LYP vertical excitation energy (T_v) values for the three states. The potential energy curves of the three states as functions of the OSO bond angle were calculated at the CASPT2/ANO-S level. In the CASPT2/ANO-S curve calculations, the OSO angle ranged from 60° to 180° and the S–O bond length value was fixed at 1.4489 Å, which is the bond length value in the CASSCF/ANO-S optimized geometry for the 1^2A_1 (\tilde{X}^2A_1) state. In all the CASPT2 calculations performed in the present work the weight values of the CASSCF reference functions in the first-order wave functions were larger than 0.87 (for the three states).

In our CASSCF calculations, eleven electrons were active and the active space included thirteen orbitals [CASSCF(11,13)]. The choice of this active space stemmed from the molecular orbital (MO) sequence in the ground-state SO_2 molecule. Based on the HF/6-31+G(*d*) calculations for the SO_2 molecule, the twelve valence molecular orbitals (MOs) are listed in the following sequence: $5a_13b_26a_14b_27a_12b_15b_21a_28a_13b_19a_110a_1$. The MOs in the sequence are given in an increasing order of the MO energy and the last three are unoccupied. Our active space was formed from the full-valence active space (see the sequence) by deleting the $5a_1$, $3b_2$, and $6a_1$ MOs (the energy gap between $6a_1$ and $4b_2$ being larger than 5 eV) and by adding four virtual MOs ($6b_2$, $4b_1$, $11a_1$, and $7b_2$) lying above $10a_1$. Labeling the orbitals within the C_{2v} point group in the order of a_1 , a_2 , b_2 , and b_1 , this active space is named (5143).

We also calculated the six lowest-lying electronic states of SO_2^+ at the linear geometry at the CASPT2/ANO-S level. The calculations were carried out in the D_{2h} group, and the calculation details will be given in Sec. III C.

We also performed DFT (density functional theory^{19,20}) B3LYP (Becke's three-parameter hybrid function²¹ with the nonlocal correlation of Lee–Yang–Parr²²) and *ab initio* MP2 (second-order Møller–Plesset perturbation theory^{23,24}) calculations for the 1^2A_1 , 1^2B_2 , and 1^2A_2 states. In these calculations we used the GAUSSIAN 98W suite of programs²⁵ and the cc-pVTZ basis set.²⁶ The UB3LYP/cc-pVTZ calculation results for 1^2A_2 are probably not so reliable since the spin contamination was relatively large ($\langle S^2 \rangle = 0.832$). In the UMP2/cc-pVTZ calculations the $\langle S^2 \rangle$ value for 1^2A_2 was as large as 1.210 and the $\langle S^2 \rangle$ value for 1^2B_2 was also quite large. We will not report the UMP2/cc-pVTZ results. The UMP method and other *ab initio* methods based on spin-unrestricted theory are not appropriate for a theoretical study of these states.

TABLE I. CASPT2/ANO-L optimized geometries for the 1^2A_1 , 1^2B_2 , and 1^2A_2 states of SO_2^+ , together with the CASSCF/ANO-L and UB3LYP/cc-pVTZ optimized geometries (bond lengths are in angstroms and angles in degrees).

State	CASSCF		UB3LYP ^a		CASPT2		Experimental ^b		
	$R(\text{S-O})$	$\angle\text{OSO}$	$R(\text{S-O})$	$\angle\text{OSO}$	$R(\text{S-O})$	$\angle\text{OSO}$		$R(\text{S-O})$	$\angle\text{OSO}$
1^2A_1	1.439	127.7	1.446	131.0	1.439	132.0	\tilde{X} :	1.432	136.5
1^2B_2	1.492	100.1	1.490	100.0	1.491	99.9	\tilde{A} :	1.432	102.5
1^2A_2	1.507	109.3	1.516	108.5	1.504	109.3			

^aSpin contamination was relatively large for the 1^2A_2 state ($\langle S^2 \rangle = 0.832$).^bReference 9, in which the bond lengths were assumed to be the same as the neutral ground state of SO_2 .

III. RESULTS AND DISCUSSION

In Table I are given the CASSCF/ANO-L, UB3LYP/cc-pVTZ, and CASPT2/ANO-L optimized geometries for the 1^2A_1 , 1^2B_2 , and 1^2A_2 states of the SO_2^+ ion. In Table II are given the CASSCF/ANO-L frequency values for the ν_1 and ν_2 modes in the three states. In Table III are given the CASPT2//CASSCF (CASPT2/ANO-L//CASSCF/ANO-L), CASPT2//UB3LYP (CASPT2/ANO-L//UB3LYP/cc-pVTZ), and CASPT2//CASPT2 (CASPT2/ANO-L//CASPT2/ANO-L) adiabatic excitation energies (T_0) and vertical excitation energies (T_v) for the 1^2A_1 , 1^2B_2 , and 1^2A_2 states of the SO_2^+ ion. These CASPT2 energetic results indicate that 1^2A_1 is the ground state (\tilde{X}^2A_1) of the SO_2^+ ion (see Sec. III B).

For confirming that the 1^2A_1 , 1^2B_2 , and 1^2A_2 states are the three lowest-lying electronic states of SO_2^+ , we calculated the CASPT2/ANO-L T_v values for the 2^2A_1 , 2^2B_2 , 2^2A_2 , and 1^2B_1 states at the CASPT2/ANO-L optimized geometry of the 1^2A_1 (\tilde{X}^2A_1) state. The calculated (CASPT2//CASPT2) T_v values for these four states were all larger than 4.4 eV and they are much higher in energy than the 1^2A_1 , 1^2B_2 , and 1^2A_2 states (see the CASPT2//CASPT2 T_v values for 1^2A_1 , 1^2B_2 , and 1^2A_2 in Table III).

A. Equilibrium geometries

In the CASPT2/ANO-L optimized geometry for the 1^2A_1 (\tilde{X}^2A_1) state the S–O bond length [$R(\text{S-O})$] and the OSO bond angle ($\angle\text{OSO}$) are 1.439 Å and 132.0°, respectively (see Table I). The bond angle value in the CASSCF/ANO-L geometry is 4.3° smaller than that in the CASPT2/ANO-L geometry. The UB3LYP/cc-pVTZ geometry [$R(\text{S-O}) = 1.446$ Å and $\angle\text{OSO} = 131.0^\circ$; $\langle S^2 \rangle = 0.757$] is similar to the CASPT2/ANO-L geometry. We believe that the UB3LYP/cc-pVTZ calculations predict reliable geometries when spin contaminations are small (for example, $\langle S^2 \rangle < 0.77$ for doublet species).

TABLE II. CASSCF/ANO-L frequency values (in cm^{-1}) for the ν_1 and ν_2 modes in the 1^2A_1 , 1^2B_2 , and 1^2A_2 states of SO_2^+ .

State	ν_1	ν_2	Experimental ^a
1^2A_1	1049.6	424.0	\tilde{X} : $\nu_1(\sim 1151)$, $\nu_2(\sim 454)$
1^2B_2	1084.6	443.9	\tilde{A} : $\nu_1(953)$, $\nu_2(499)$
1^2A_2	1032.2	467.8	

^aReference 7.

In the CASPT2/ANO-L optimized geometry for the 1^2B_2 state the S–O bond length and the OSO bond angle are 1.491 Å and 99.9°, respectively (see Table I). The CASSCF/ANO-L geometry [$R(\text{S-O}) = 1.492$ Å and $\angle\text{OSO} = 100.1^\circ$] and the UB3LYP/cc-pVTZ geometry [$R(\text{S-O}) = 1.490$ Å and $\angle\text{OSO} = 100.0^\circ$; $\langle S^2 \rangle = 0.761$] are almost identical to the CASPT2/ANO-L geometry. In the CASPT2/ANO-L optimized geometry for the 1^2A_2 state the S–O bond length and the OSO bond angle are 1.504 Å and 109.3°, respectively (see Table I). The CASSCF/ANO-L geometry [$R(\text{S-O}) = 1.507$ Å and $\angle\text{OSO} = 109.3^\circ$] is almost identical to the CASPT2/ANO-L geometry. The UB3LYP/cc-pVTZ geometry [$R(\text{S-O}) = 1.516$ Å and $\angle\text{OSO} = 108.5^\circ$; $\langle S^2 \rangle = 0.832$] is quite close to the CASPT2/ANO-L geometry though the spin contamination was relatively large.

It is noted that the CASPT2/ANO-L geometry for the 1^2A_1 (\tilde{X}^2A_1) state is significantly different from the experimental geometry for the \tilde{X} state and the CASPT2/ANO-L geometries for the 1^2B_2 and 1^2A_2 states are both far from the experimental geometry for the \tilde{A} state. We realize that those experimental geometries⁹ for the \tilde{X} and \tilde{A} states of SO_2^+ were not accurately determined, and it is not possible to assign the \tilde{A} state of SO_2^+ (to 1^2B_2 or 1^2A_2) based on the calculation results for geometries. The previous RHF calculations¹⁰ predicted a S–O bond length value of 1.501 Å for the 1^2A_1 state, which is much larger than the CASPT2/ANO-L value. The RHF geometries¹⁰ for the 1^2B_2 [$R(\text{S-O}) = 1.553$ Å and $\angle\text{OSO} = 104.7^\circ$] and 1^2A_2 [$R(\text{S-O}) = 1.571$ Å and $\angle\text{OSO} = 108.8^\circ$] states are significantly different from the CASPT2/ANO-L geometries for the respective states (the RHF bond lengths were too long).

The experimental frequency values for the ν_1 and ν_2 vibrational modes in the \tilde{X} and \tilde{A} states of SO_2^+ were reported in several papers (see Ref. 7, and references therein). We calculated the ν_1 and ν_2 frequency values in the 1^2A_1 , 1^2B_2 , and 1^2A_2 states of SO_2^+ at the CASSCF/ANO-L level using the MCLR program of the MOLCAS software. The calculated ν_1 (1049 cm^{-1}) and ν_2 (424 cm^{-1}) values in the 1^2A_1 state are slightly smaller than the experimental ν_1 (1151 cm^{-1}) and ν_2 (454 cm^{-1}) values in the \tilde{X} state,⁷ respectively. The calculated ν_1 values in the 1^2B_2 and 1^2A_2 states are similar and they are slightly larger than the experimental ν_1 value in the \tilde{A} state; and the calculated ν_2 values in the 1^2B_2 and 1^2A_2 states are also similar and they are slightly smaller than the experimental ν_2 value in the \tilde{A} state.

TABLE III. CASPT2 adiabatic (T_0) and vertical (T_v) excitation energies (in eV) for the 1^2A_1 , 1^2B_2 , and 1^2A_2 states of SO_2^+ calculated using the CASSCF, UB3LYP, and CASPT2 optimized geometries, together with the CASSCF and UB3LYP adiabatic excitation energies.^a

	State	CASSCF	UB3LYP ^b	CASPT2			Experimental ^c
				//CASSCF	//UB3LYP	//CASPT2	
T_0	1^2A_1	0.00	0.00	0.00	0.00	0.00	0.00
	1^2B_2	-0.06	0.34	0.54	0.56	0.56	\tilde{A} : 0.64
	1^2A_2	0.03	0.84 ^b	1.20	1.21	1.21	\tilde{B} : 0.99
T_v	1^2A_1			0.00	0.00	0.00	
	1^2B_2			1.52	1.69	1.79	
	1^2A_2			1.82	1.95	2.04	

^aThe ANO-L basis was used in the CASSCF and CASPT2 calculations and the cc-pVTZ basis was used in the UB3LYP calculations.

^bSpin contamination was relatively large for the 1^2A_2 state ($\langle S^2 \rangle = 0.832$).

^cEvaluated using the experimental adiabatic ionization potential data reported in Ref. 2.

(see Table II). It is not possible to assign the \tilde{A} state of SO_2^+ (to 1^2B_2 or 1^2A_2) based on the calculation results for frequencies.

B. Adiabatic and vertical excitation energies

The CASPT2//CASSCF, CASPT2//UB3LYP, and CASPT2//CASPT2 adiabatic excitation energy (T_0) values for the 1^2A_1 , 1^2B_2 , and 1^2A_2 states of the SO_2^+ ion (see Table III) indicate that the 1^2A_1 state is the ground state (\tilde{X}^2A_1) of SO_2^+ and that 1^2B_2 and 1^2A_2 are the first and second excited states, respectively. At the CASPT2//CASPT2 level the T_0 values for the 1^2B_2 and 1^2A_2 states are predicted to be 0.56 and 1.21 eV, respectively. The CASPT2//CASSCF and CASPT2//UB3LYP T_0 values for the 1^2B_2 and 1^2A_2 states are very close to the CASPT2//CASPT2 values for the respective states. The experimental T_0 values for the \tilde{A} and \tilde{B} states of the SO_2^+ ion are evaluated to be 0.64 and 0.99 eV, respectively, based on the experimental AIP data.² The CASPT2//CASPT2 T_0 value of 0.56 eV for 1^2B_2 is 0.06 eV smaller than the experimental T_0 value for the \tilde{A} state and the CASPT2//CASPT2 T_0 value of 1.21 eV for 1^2A_2 is 0.22 eV larger than the experimental T_0 value for the \tilde{B} state. We assign the \tilde{A} state of SO_2^+ to 1^2B_2 and the \tilde{B} state to 1^2A_2 . These assignments based on the CASPT2//CASPT2 T_0 values are unambiguous, since the smaller one of the two calculated T_0 values is smaller than the smaller one of the two experimental T_0 values and the larger one of the two calculated T_0 values is larger than the larger one of the two experimental T_0 values. We consider that the deviation of 0.06 eV is small and the deviation of 0.22 eV is not large. Our assignments of the \tilde{A} and \tilde{B} states of SO_2^+ (\tilde{A} to 1^2B_2 and \tilde{B} to 1^2A_2) are contrary to the assignments (\tilde{A} to 1^2A_2 and \tilde{B} to 1^2B_2) presented in the previous experimental papers²⁻⁷ based on the energy ordering of the three highest occupied molecular orbitals in the electronic structure of the ground-state SO_2 molecule and in the previous theoretical paper¹⁰ based on the RHF calculations.

The CASPT2//CASSCF, CASPT2//UB3LYP, and CASPT2//CASPT2 vertical excitation energy (T_v) values for the 1^2A_1 , 1^2B_2 , and 1^2A_2 states of the SO_2^+ ion (see Table

III) indicate that the 1^2B_2 and 1^2A_2 states are the first and second excited states, respectively, at the ground-state (1^2A_1) geometry of the SO_2^+ ion. At the CASPT2//CASPT2 level the T_v values for the 1^2B_2 and 1^2A_2 states are predicted to be 1.79 and 2.04 eV, respectively. The CASPT2//CASSCF and CASPT2//UB3LYP T_v values for the 1^2B_2 and 1^2A_2 states are smaller than the CASPT2//CASPT2 values for the respective states (see Table III). Experimental data for the vertical excitation energies are not available. We also performed the CASPT2/ANO-L energetic calculations for the three states of SO_2^+ at the experimental geometry²⁷ [$R(\text{S-O}) = 1.432 \text{ \AA}$ and $\angle \text{OSO} = 119.5^\circ$] of the ground-state SO_2 molecule, and the relative energies for the 1^2A_1 , 1^2B_2 , and 1^2A_2 states are 0.00, 1.01, and 1.45 eV, respectively. These values indicate that the 1^2A_1 , 1^2B_2 , and 1^2A_2 states are the ground state, the first excited state, and the second excited states of SO_2^+ , respectively, at the geometry of the ground-state SO_2 molecule. It is noted that the energy ordering (1^2A_1 , 1^2B_2 , and 1^2A_2) for the three states at the geometry of the ground-state SO_2 molecule indicated by the CASPT2/ANO-L calculations is not the same as the ordering ($2A_1$, $2A_2$, and $2B_2$) indicated by the Green's function calculations.¹¹

The CASSCF (CASSCF/ANO-L//CASSCF/ANO-L) and UB3LYP (UB3LYP/cc-pVTZ//UB3LYP/cc-pVTZ) adiabatic excitation energy values for the 1^2A_1 , 1^2B_2 , and 1^2A_2 states are also given in Table III. The CASSCF T_0 values (-0.06 and 0.03 eV for 1^2B_2 and 1^2A_2 , respectively) are very small and they are far from the CASPT2//CASSCF (and CASPT2//CASPT2) values and from the experimental values, which indicates that dynamic electron correlation effects are important in these states. Though the UB3LYP T_0 values (0.34 and 0.84 eV for 1^2B_2 and 1^2A_2 , respectively) are not in very good agreement with the experimental values and there was relatively large spin contamination for the 1^2A_2 state, the UB3LYP/cc-pVTZ adiabatic excitation energy calculations support the assignments (\tilde{X} , \tilde{A} , and \tilde{B} states to 1^2A_1 , 1^2B_2 , and 1^2A_2 , respectively) based on the CASPT2/ANO-L calculations.

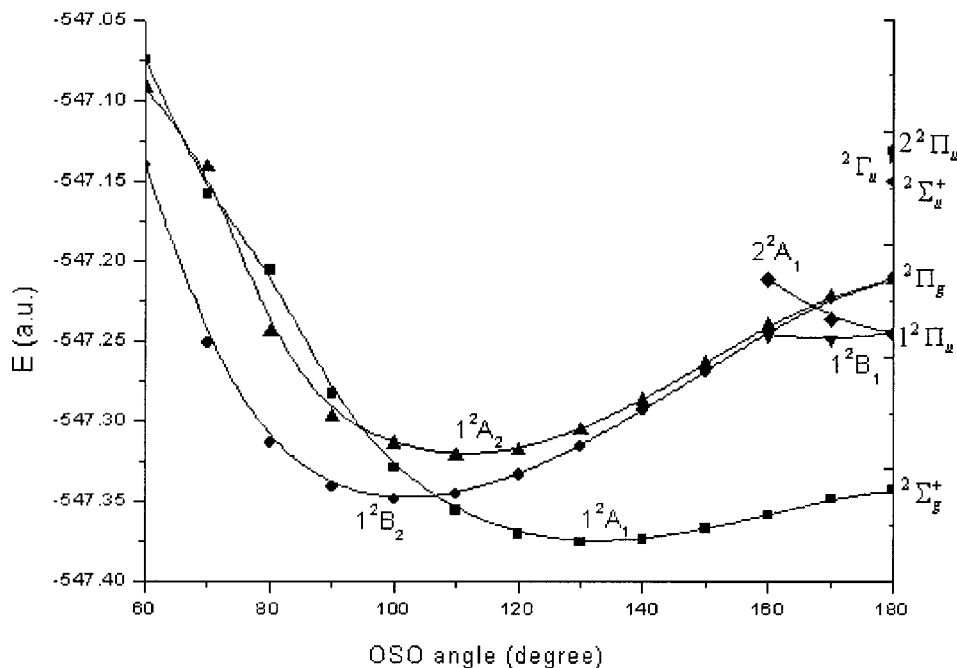


FIG. 1. CASPT2/ANO-S potential energy curves for the 1^2A_1 , 1^2B_2 , and 1^2A_2 states of SO_2^+ , as functions of the OSO bond angle.

C. Potential energy curves

The CASPT2/ANO-S potential energy curves for the 1^2A_1 , 1^2B_2 , and 1^2A_2 states of SO_2^+ , as functions of the OSO bond angle, are given in Fig. 1. The minima along the 1^2A_1 , 1^2B_2 , and 1^2A_2 curves were located at the OSO bond angle values of 133° , 102° , and 112° , which are quite close to the bond angle values in the CASPT2/ANO-L geometries (see Table I) of the 1^2A_1 , 1^2B_2 , and 1^2A_2 states, respectively. The relative values (0.00, 0.76, and 1.51 eV) for the CASPT2/ANO-S energies at these minima are in the order of 1^2A_1 , 1^2B_2 , and 1^2A_2 , and at the OSO angle values of 133° (see above) and 119.5° (the experimental bond angle value for the ground-state SO_2 molecule²⁷) the 1^2A_1 state is the lowest-lying state and the 1^2B_2 state lies below 1^2A_2 . These facts are in line with the CASPT2/ANO-L energetic results reported in Sec. III B. It is noted that the 1^2B_2 state is lower in energy than 1^2A_1 when the OSO angle is smaller than 106° .

Low-lying electronic states of the SO_2^+ ion at the linear geometry with the S–O bond length of 1.4489 Å (see Sec. II) were calculated at the CASPT2/ANO-S level. The calculations were carried out in the D_{2h} subgroup of $D_{\infty h}$, where Σ_g^+ corresponds to the A_g irreducible representation, Σ_u^+ to B_{1u} , Π_g to $B_{2g}+B_{3g}$, Π_u to $B_{2u}+B_{3u}$, and Γ_u to A_u+B_{1u} . The CASPT2 calculations in the D_{2h} point group were still based on the CASSCF(11,13) calculations (eleven electrons were active and the active space included thirteen orbitals, see Sec. II). Labeling the orbitals within the D_{2h} point group in the order of a_g , b_{3u} , b_{2u} , b_{1g} , b_{1u} , b_{2g} , b_{3g} , and a_u , an active space named (23302210) was used. It is equivalent to the (5143) active space (labeling the orbitals within the C_{2v} point group, see Sec. II). In the CASSCF calculation steps of our CASPT2/ANO-S calculations for the electronic states at the linear geometry, the state-averaging technique was used. The averaging includes all the states of interest for a given symmetry of the D_{2h} group.

Our CASPT2/ANO-S calculations predict that the $2^2\Sigma_g^+$, $(1)^2\Pi_u$, $2^2\Pi_g$, $2^2\Sigma_u^+$, $2^2\Gamma_u$, and $(2)^2\Pi_u$ states (see Fig. 1) are the six lowest-lying states of the SO_2^+ ion at the linear geometry, and the CASPT2/ANO-S relative energies for these states are 0.0, 2.66, 3.59, 5.24, 5.65, and 5.73 eV, respectively. In Fig. 1 the following state-correlations are shown: the 1^2A_1 (\tilde{X}^2A_1) curve converges to the $(\tilde{X})^2\Sigma_g^+$ state at the linear geometry; both the 1^2B_2 and 1^2A_2 curves converge to the degenerate $2^2\Pi_g$ state, which is the third lowest-lying state at the linear geometry; and the second lowest-lying state [$(1)^2\Pi_u$] is correlated to 1^2B_1 and 2^2A_1 , which are high-lying states at the ground-state (\tilde{X}^2A_1) geometry of the SO_2^+ ion (see the beginning of Sec. III).

The 1^2B_2 and 1^2A_2 states are considered as the results of the Renner–Teller effect²⁸ in the degenerate $2^2\Pi_g$ state. Since each of the 1^2B_2 and 1^2A_2 states has one minimum at an OSO angle value not equal to 180° , the Renner-splitting pattern for the $2^2\Pi_g$ state is pattern (c) of Pople and Longuet-Higgin’s scheme.²⁹ The most important fact shown in Fig. 1 is that the curve for the 1^2B_2 state (the lower component of the Renner splitting) lies below the curve for the 1^2A_2 state (the upper component). The 1^2B_1 and 2^2A_1 states are the results of the Renner–Teller effect in the $(1)^2\Pi_u$ state, and we will not discuss them in the present paper.

IV. CONCLUSIONS

The three lowest-lying electronic states of the SO_2^+ ion, 1^2A_1 , 1^2B_2 , and 1^2A_2 , were studied using the CASPT2 method and two contracted ANO basis sets, $S[6s4p3d1f]/O[5s3p2d1f]$ (ANO-L) and $S[4s3p2d]/O[3s2p1d]$ (ANO-S).

The CASPT2/ANO-L geometries for the 1^2A_1 [$R(\text{S–O})=1.439$ Å and $\angle\text{OSO}=132.0^\circ$], 1^2B_2 [$R(\text{S–O})=1.491$ Å and $\angle\text{OSO}=99.9^\circ$], and 1^2A_2 [$R(\text{S–O})$

$=1.504 \text{ \AA}$ and $\angle \text{OSO}=109.3^\circ$] states are compared with the experimental geometries for the \tilde{X} [$R(\text{S-O})=1.432 \text{ \AA}$ and $\angle \text{OSO}=136.5^\circ$] and \tilde{A} [$R(\text{S-O})=1.432 \text{ \AA}$ and $\angle \text{OSO}=102.5^\circ$] states. We realize that the experimental geometries (reported in Ref. 9) for the \tilde{X} and \tilde{A} states of the SO_2^+ ion were not accurately determined since the bond length values were assumed to be 1.432 \AA . The CASSCF/ANO-L frequency calculations predict similar ν_1 values and similar ν_2 values for the 1^2B_2 and 1^2A_2 states. It is not possible to assign the \tilde{A} state of SO_2^+ (to 1^2B_2 or 1^2A_2) based on the calculation results for geometries and vibrational frequencies.

Based on the CASPT2/ANO-L T_0 calculations, the observed \tilde{X} , \tilde{A} , and \tilde{B} states of the SO_2^+ ion are assigned to 1^2A_1 , 1^2B_2 , and 1^2A_2 , respectively. The CASPT2//CASPT2 T_0 values of 0.56 and 1.21 eV for 1^2B_2 and 1^2A_2 are in reasonable agreement with the experimental values of 0.64 and 0.99 eV (based on the experimental AIP data) for the \tilde{A} and \tilde{B} states, respectively. Our assignments of the \tilde{A} and \tilde{B} states (\tilde{A} to 1^2B_2 and \tilde{B} to 1^2A_2) are contrary to the assignments (\tilde{A} to 1^2A_2 and \tilde{B} to 1^2B_2) presented in the previous experimental papers based on the energy ordering of the three highest occupied molecular orbitals in the electronic structure of the ground-state SO_2 molecule and in the previous theoretical paper based on the RHF calculations. The CASPT2/ANO-L energetic calculations also indicate that the 1^2A_1 , 1^2B_2 , and 1^2A_2 states are, respectively, the ground, first excited, and second excited states of SO_2^+ at the ground-state (1^2A_1) geometry of the ion and at the geometry of the ground-state SO_2 molecule.

The potential energy curves for the 1^2A_1 , 1^2B_2 , and 1^2A_2 states of SO_2^+ were calculated as functions of the OSO angle (ranging from 60° to 180°) at the CASPT2/ANO-S level, and the six lowest-lying states of SO_2^+ at the linear geometry were also calculated at the same level. These CASPT2/ANO-S calculations confirm that the 1^2B_2 and 1^2A_2 states are the results of the Renner–Teller effect in the degenerate $2\Pi_g$ state at the linear geometry, and it is clearly shown that the curve for the 1^2B_2 state (the lower component of the Renner splitting) lies below the curve for the 1^2A_2 state (the upper component).

The UB3LYP/cc-pVTZ calculations were performed for the 1^2A_1 , 1^2B_2 , and 1^2A_2 states of SO_2^+ (spin contamination for 1^2A_2 was relatively large). The UB3LYP/cc-pVTZ geometries for the three states are similar to the CASPT2/ANO-L geometries for the respective states. The UB3LYP/cc-pVTZ adiabatic excitation energy calculations support the assignments (\tilde{X} to 1^2A_1 , \tilde{A} to 1^2B_2 , and \tilde{B} to 1^2A_2) based on the CASPT2/ANO-L calculations. The UMP2 method is not appropriate for a theoretical study of these states due to large spin contaminations for 1^2A_2 and 1^2B_2 . The CASSCF calculations predict no good results for the T_0 values, which

indicates that dynamic electron correlation effects are important in these states.

Theoretical study for higher-lying states in the third band (\tilde{C} , \tilde{D} , and \tilde{E}) of the photoelectron spectrum of SO_2^+ is in progress. Preliminary CAS calculations indicate that in that energy region there may be more states including shake-up ionized states.

ACKNOWLEDGMENTS

This work was supported by the National Natural Science Foundation Committee of China (No. 20173056, 20333050) and the Ministry of Science and Technology of China (No. G199907530).

- ¹Molecular Ions: Geometric and Electronic Structures, edited by J. Berkowitz and K. O. Groenfeld (Plenum, New York, 1983).
- ²L. Wang, Y. T. Lee, and D. A. Shirley, J. Chem. Phys. **87**, 2489 (1987).
- ³D. M. P. Holland, M. A. MacDonald, M. A. Hayes, P. Baltzer, L. Karlsson, M. Lundqvist, B. Wannberg, and W. von Niession, Chem. Phys. **188**, 317 (1994).
- ⁴R. Basner, M. Schmidi, H. Deutsch, V. Tarnovsky, A. Levin, and K. Becker, J. Chem. Phys. **103**, 211 (1995).
- ⁵G. Dujardin and S. Leach, J. Chem. Phys. **75**, 2521 (1981).
- ⁶M. J. Weiss, Ta-Cheng Hsieh, and G. G. Meisels, J. Chem. Phys. **71**, 567 (1979).
- ⁷T. F. Thomas, F. Dale, and J. F. Paulson, J. Chem. Phys. **84**, 1215 (1986), and references therein.
- ⁸L. Zhang, Z. Wang, J. Li, F. Wang, S. Liu, S. Yu, and X. Ma, J. Chem. Phys. **118**, 9185 (2003).
- ⁹J. H. D. Eland and C. J. Danby, Int. J. Spectromet. Ion Phys. **1**, 111 (1968).
- ¹⁰I. H. Hillier and V. R. Saunders, Mol. Phys. **22**, 193 (1971).
- ¹¹L. S. Cederbaum, W. Domcke, W. V. Niessen, and W. P. Kraemer, Mol. Phys. **34**, 381 (1977).
- ¹²B. O. Roos, in *Ab Initio Methods in Quantum Chemistry*, Part 2, edited by K. P. Lawley (Wiley, New York, 1987).
- ¹³K. Andersson, P.-A. Malmqvist, B. O. Roos, A. J. Sadley, and K. Wolinski, J. Phys. Chem. **94**, 5483 (1990).
- ¹⁴K. Andersson, P.-A. Malmqvist, and B. O. Roos, J. Chem. Phys. **96**, 1218 (1992).
- ¹⁵K. Andersson, M. P. Fulscher, R. Lindh, P.-A. Malmqvist, J. Olsen, A. J. Sadley, and P.-O. Widmark, MOLCAS (version 5.2), University of Lund, Sweden, 2002.
- ¹⁶J. Almlöf and P. R. Taylor, J. Chem. Phys. **86**, 4070 (1987).
- ¹⁷P.-O. Widmark, P.-A. Malmqvist, and B. O. Roos, Theor. Chim. Acta **77**, 291 (1990).
- ¹⁸P.-O. Widmark, B.-J. Persson, and B. O. Roos, Theor. Chim. Acta **79**, 419 (1991).
- ¹⁹P. Hohenberg and W. Kohn, Phys. Rev. **136**, B864 (1964).
- ²⁰W. Kohn and L. J. Sham, Phys. Rev. **140**, A1133 (1965).
- ²¹A. D. Becke, J. Chem. Phys. **98**, 5648 (1993).
- ²²C. Lee, W. Yang, and R. G. Parr, Phys. Rev. B **37**, 785 (1988).
- ²³C. Möller and M. S. Plesset, Phys. Rev. **46**, 618 (1934).
- ²⁴J. A. Pople, J. S. Binkley, and R. Seeger, Int. J. Quantum Chem. **10**, 1 (1976).
- ²⁵M. J. Frish, G. W. Trucks, H. B. Schlegel *et al.*, GAUSSIAN 98, Revision D.1, Gaussian, Inc., Pittsburgh, PA, 1998.
- ²⁶D. E. Woon and T. H. Dunning, Jr., J. Chem. Phys. **98**, 1358 (1993).
- ²⁷D. Kivelson, J. Chem. Phys. **22**, 904 (1954).
- ²⁸R. Renner, Z. Phys. **92**, 172 (1934).
- ²⁹J. A. Pople and H. C. Longuet-Higgins, Mol. Phys. **1**, 372 (1958).